Cell Tissue Res (2013) 352:671–684
DOI 10.1007/s00441-013-1608-8

REGULAR ARTICLE

Breast cancer tissue slices as a model for evaluation of response to rapamycin

Stana Helena Giorgi Grosso · Maria Lucia Hirata Katayama · Rosimeire Aparecida Roela · Suely Nonogaki · Fernando Augusto Soares · Helena Brentani · Leandro Lima · Maria Aparecida Azevedo Koike Folgueira · Angela Flávia Logullo Waitzberg · Fátima Solange Pasini · João Carlos Guedes Sampaio Góes · M. Mitzi Brentani

Received: 12 July 2012 / Accepted: 4 March 2013 / Published online: 1 May 2013

Abstract Rapamycin is a selective inhibitor of the mammalian target of rapamycin (mTOR), a regulator kinase that integrates growth factors signaling via the phosphoinositide-3-kinase pathway and that has emerged as a novel therapeutic modality in breast cancer (BC). We propose a pre-clinical "ex-vivo" personalized organotypic culture of BC that preserves the microenvironment to evaluate rapamycin-mediated gene expression changes. Freshly excised ductal invasive BC slices, 400 μm thick (n=30), were cultured in the presence or absence (control) of rapamycin (20 nM) for 24 h. Some slices were formalin-fixed for immunohistochemical determinations and some were processed for microarray analysis. Control slices in culture retained their tissue morphology and tissue viability (detected by BrdU uptake). The percentage of proliferating cells (assessed by Ki67) did not change up to 24 h of treatment. Immunohistochemical evaluation of p-AKT, p-mTOR, p-4EBP1 and p-S6K1 indicated that AKT/mTOR pathway activation was maintained during cultivation. For microarray

S.H.G.G., M.L.H.K. and R.A.R. contributed equally to this work.

This work was supported by FAPESP 2009/10088-7 and CNPQ.

The authors declare that they have no competing interests.

Electronic supplementary material The online version of this article (doi:10.1007/s00441-013-1608-8) contains supplementary material, which is available to authorized users.

S. H. G. Grosso · J. C. G. S. Góes
Instituto Brasileiro de Controle do Câncer,
Av. Alcântara Machado 2576,
CEP 03102-002 São Paulo, SP, Brasil

M. L. H. Katayama · R. A. Roela · M. A. A. K. Folgueira · F. S. Pasini · M. M. Brentani (✉)
Departamento de Radiologia e Oncologia, Disciplina de Oncologia (LIM-24), Faculdade de Medicina da Universidade de São Paulo,
Av. Dr. Arnaldo 455, Sala 4123,
CEP 01246-903 São Paulo, SP, Brasil
e-mail: mbrentani@lim24.fm.usp.br

S. Nonogaki
Central, Divisão de Patologia, Laboratório de Imuno-histoquímica,
Instituto Adolfo Lutz,
Av. Dr. Arnaldo 355, 7º Andar Cerqueira César,
CEP 01246-902 São Paulo, SP, Brazil

F. A. Soares
Hospital A C Camargo, Rua Professor Antônio Prudente 211,
01509-010 São Paulo, Brasil

H. Brentani
Departamento de Psiquiatria (LIM-23), Faculdade de Medicina da Universidade de São Paulo, Rua Ovideo Pires de Campos S/Nº,
São Paulo, Brasil

L. Lima
Laboratório de Bioinformática e Bioestatística, Centro Internacional de Pesquisa e Ensino (CIPE), Hospital AC Camargo,
Rua Taguá 440,
CEP 01508-010 São Paulo, Brazil

A. F. L. Waitzberg
Departamento de Patologia, Universidade Federal de São Paulo,
Rua Botucatu 740,
CEP 04023-900 São Paulo, Brasil

analysis, slices were divided into two groups, according to the presence/absence of epidermal growth factor receptor-type 2 and analyzed separately. Limited overlap was seen among differentially expressed genes after treatment ($P<0.01$) in both groups suggesting different responses to rapamycin between these BC subtypes. Ontology analysis indicated that genes involved in biosynthetic processes were commonly reduced by rapamycin. Our network analysis suggested that concerted expression of these genes might distinguish controls from treated slices. Thus, breast carcinoma slices constitute a suitable physiological tool to evaluate the short-term effects of rapamycin on the gene profile of individual BC samples.

Keywords Breast cancer · Rapamycin · Ex-vivo model · AKT/mTOR pathway · Co-expression network · Human

Introduction

The mammalian target of rapamycin (mTOR) is an important regulatory kinase that integrates upstream signals from growth factors, amino-acid availability and stresses into processes such as regulated cell growth, survival, proliferation, cell metabolism and angiogenesis. mTOR is the catalytic subunit of two multiprotein complexes, namely mTORC-1 and mTORC-2, the first being a major driver of cell growth and protein translation and the latter being involved in less defined functions, probably including actin cytoskeleton and cell survival. In particular, the PI3K (phosphoinositide-3-kinase)-AKT (also known as protein kinase B) pathway and the Ras-ERK (extracellular-signal-regulated kinase) pathway are stimulated by mTORC-1 signaling (Guertin and Sabatini 2007).

Activation of mTORC-1 results in the phosphorylation of its downstream targets including p70 ribosomal protein S6 kinase (S6K1) and the eukaryotic initiation factor 4E-binding protein 1 (4EBP1). S6K1 recruits the 40S ribosomal protein S6, which upon phosphorylation promotes the translation of mRNAs that bear a 5'-terminal oligopyrimidine, including mRNAs that encode for ribosomal proteins and elongation factors. Phosphorylation of 4EBP1 by mTORC-1 induces its dissociation from the eukaryotic initiation factor-4 subunit complex (eIF-4E) and increased free eIF-4E enhances cap-dependent translation of numerous mRNAs, resulting in the activation of cell protein synthesis and cell growth (Zoncu et al. 2011; Hernandez-Aya and Gonzalez-Angulo 2011). Increasing evidence suggests that this pathway is frequently deregulated in breast carcinoma and thus mTOR is considered a therapeutic target (Dillon et al. 2007).

Rapamycin is an antibiotic and fungicide that predominantly inhibits mTORC-1 function leading therefore to the dephosphorylation of S6K1 and 4EBP1 and inhibiting, in turn, the translation of specific mRNAs involved in cell proliferation. Rapamycin and its analogs have emerged as a novel potential therapeutic modality for breast cancer by themselves or in combination with other chemotherapy drugs. Clinical trials with mTOR antagonists are currently underway to test the efficacy of the treatment but only a fraction of patients respond to the drug and the identification of potential predictors of sensitivity to rapamycin treatment is being pursued (Zoncu et al. 2011; Meric-Bernstam and Gonzalez-Angulo 2009). The reduced phosphorylation status of AKT, S6K1 and 4EBP1 in clinical breast cancer samples and cell lines has been proposed as a possible determinant of sensitivity to the drug by some authors but such results have not been confirmed by others (Dudkin et al. 2001; Noh et al. 2004; Zhou et al. 2004; Yu et al. 2001; Satheesha et al. 2011). A pre-operative study of patients receiving a rapamycin analog (RAD001) for 2 weeks has reported that tumors with high Ki67, p-AKT and epidermal growth factor receptor-type 2 (HER2)-positive levels might be more responsive to mTORC-1 inhibition with the drug (Macaskill et al. 2011).

A few studies have been performed on breast cancer cell lines (Heinonen et al. 2008; Akcakanat et al. 2009) to analyze the transcriptional effects of rapamycin; however, the contribution of the microenvironment to the regulation of signal transduction in cancer cells (Rozenchan et al. 2009), as possibly having an important impact in the success of chemotherapy (Finak et al. 2008), has not been evaluated. A recent study has reported the characterization of the effects of a rapamycin analog (everolimus) as a single agent on tumor gene expression in matched pre- and post-treatment samples after 11 days of treatment (Sabine et al. 2010).

Because of the high cellular heterogeneity of breast carcinoma and the heterogeneity among patients, a more physiological experimental approach is needed to analyze individual patient responses to the drug. The use of an "ex-vivo" model of organoid cultures has great potential in the study of tumor responses to anti-cancer drugs, as the complex interacting network of tumor and stromal cells and extracellular matrix (ECM) is maintained. The purpose of the present study is two-fold: (1) to examine the reliability of using "ex-vivo" breast cancer tissue slices in culture as a model to evaluate early genes regulated by rapamycin in individual breast cancer samples that might represent potential intervention targets; (2) to verify whether breast cancer slices maintain the activation status of the downstream elements of the AKT/mTOR pathway as determined by immunohistochemistry.

Materials and methods

Patients

In total, 30 patients admitted to the Instituto Brasileiro de Controle do Câncer (São Paulo, Brazil) for mastectomy as a

breast cancer treatment were included in the present study, each patient providing written informed consent. This study was approved by the Institutional Ethics Committee. Clinical and histopathological characteristics were recorded at the time of primary surgery according to the standard diagnostic classification. The age of the patients ranged from 30 to 80 years; 70% were aged≥50 years and tumor size ranged from 3 to 8 cm. All the patients had infiltrating ductal carcinomas; 87% were clinically staged as IIB and IIIB and only 13% as IIA. HER overexpressing tumors (scoring +3 by immunohistochemistry) constituted 43.3% of the tumors. Estrogen receptor (ER) and progesterone receptor (PR) were positive in 56.7% of tumors. Three patients (one HER-positive and two HER-negative) were further included only for analysis by real-time reverse transcription with the polymerase chain reaction (RT-PCR), after providing written informed consent.

Tissue slice preparation and culture

Primary breast tumors larger than 3 cm were collected immediately after surgical resection and transported to the laboratory in ice-cold culture medium, namely Dulbecco's modified Eagle's medium (DMEM) with antibiotics and fungicide but lacking growth factors. Time from harvest after surgery to tumor slicing was kept to an absolute minimum (<2 h). The tissue slice procedure and culture conditions followed previously published methods (Mira-y-Lopez et al. 1991; Bläuer et al. 2008; Stoff-Khalili et al. 2005; Barbosa et al. 2004; Sobral et al. 2008; Vaira et al. 2010; Milani et al. 2010). Briefly, tissue slices with a thickness of 400 μm according to the protocol of Vaira et al. 2010 were prepared by using a precision cutting tissue slicer (Krumdieck, Alabama Research and Development, Munsford, USA). On average, 12–20 slices were prepared from each tumor and kept in serum supplemented with ice-cold culture medium. Some slices from each specimen were harvested at baseline time (T0), fixed in 10% buffered formalin and used for confirmation of the histopathological diagnosis of invasive breast ductal carcinoma and for preculture immunohistochemical analyses. The remaining slices were cultured for 24 h in 6-well plates (1 slice/well) containing 2 ml culture medium (RPMI 1640 supplemented with 10% bovine fetal serum, 5 μg/ml insulin, 1% glutamine, 100 μg/ml ampicilin, 100 mg/ml streptomycin, 10 ng/ml epithelial growth factor, 500 ng/ml hydrocortisone) in the absence (control) or presence of rapamycin (20 nM) obtained from LC Laboratories, a Division of PKC Pharmaceutics (Woburn, Mass., USA). Slices were maintained at 37°C in a humidified atmosphere of 95% air, 5% CO_2 for 24 h. Some of the tissue slices of each group (control and treated) were fixed in buffered formalin after 24 h of culture and submitted to immunohistochemical analysis. The remaining slices were then cryopreserved in liquid nitrogen for molecular analysis. Cell viability was evaluated by using 5-bromo-2′-deoxyuridine (BrdU) incorporation as previously described (Milani et al. 2010).

Immunohistochemical staining

At first, in order to evaluate tissue morphology in tumor samples submitted to culture conditions, formalin-fixed paraffin-embedded tissue slice sections (3 μm) were stained with hematoxylin/eosin before (T0) and after in vitro culture for 24 h in medium without rapamycin (control). Infiltrative carcinomas were represented in all samples analyzed, as verified by histological analysis. ER, PR and HER2 were assessed only at T0. We further evaluated p-AKT, p-mTOR and the downstream intermediates p-4EBP1 and p-S6K1 by using phospho-specific antibodies, all purchased from Cell Signaling Technology: phospho-AKT (specifically phosphorylation of threonine 308; 244F9H2), rabbit monoclonal antibody (no. 9266) at a dilution of 1:50; phospho-4EBP1 (Thr 37/46), rabbit monoclonal antibody (no. 2855) diluted 1:100; phospho-mTOR (serine 2498; 49 F9), rabbit monoclonal antibody (no. 2976) diluted 1:800; phospho-S6K1 (Thr389), rabbit monoclonal antibody (no. 9206) diluted 1:200. Slides processed with normal rabbit serum in place of the primary antibody were used as negative controls and were included in each batch for immunohistochemistry. Slides of tissues known to express p-AKT, p-mTOR, p-S6K1 and p-4EBP1 were used as positive controls. Monoclonal antibody to ER (clone 6 F-11, diluted 1:50) was obtained from Neomarkers; PR (mouse monoclonal, PgR636, diluted 1:200), HER2 (polyclonal, diluted 1:1000) and Ki67 (MIB-1, diluted 1:50) were purchased from Dako, Carpinteria, Calif., USA). p-AKT, p-mTOR, p-S6K1, p-4EBP1 and Ki67 were assessed at the start of the experiment (T0) and after 24 h of cultivation in the presence or absence of rapamycin.

Briefly, after deparaffinization and rehydratation, 3-μm-thick sections were subjected to heat-induced epitope retrieval in 10 nM citrate buffer (pH6.0). Endogenous peroxidase activity was blocked in 3% H_2O_2. Slides were incubated with primary antibody for 18 h at 4°C in a humidified chamber and then incubated with a Post Primary Block (Novolink Max Polymer no. RE7260-k, UK) for 30 min at 37°C followed by washes with phosphate-buffered saline and incubation with a Novolink Polymer for 30 min at 37°C. Next, 3-3′-diaminobenzidine was used for color development and hematoxylin was used for counter staining.

If at least 10% of the tumor cells were stained with the specific antibody, the sample was considered as positive for the expression of that phosphorylated protein. In addition, immunohistochemical staining for the phosphoproteins was evaluated by a semi-quantitative scoring system: 0=<10% stained tumor cells; 1+= 10%–20% stained tumor cells; 2+= 21%–50% stained tumor cells, 3+ =>51% stained tumor cells. Based on this system, differential expression of the proteins in

paired samples (in the presence or absence of rapamycin) was evaluated. Ki67 was scored as positive if the tumor displayed≥10% stained tumor cells.

Microarray analysis

Total RNA extracted by TRIZOL reagent (Invitrogen, Carlsbad, Calif., USA) was purified with RNeasy minicolumns and reagents from Qiagen (Hilden, Germany). RNA microarray analysis was performed with 10 μg biotin-labeled cRNA target prepared by a linear amplification method. The poly(A)$^+$ RNA (mRNA) subpopulation within the total RNA population was primed for reverse transcription by a DNA oligonucleotide containing the T7 RNA polymerase promoter 5′ to a $d(T)_{24}$ sequence. After second-strand cDNA synthesis, the cDNA served as the template for an in vitro transcription reaction to produce the target cRNA. This cRNA was hybridized by using CodeLink Human Whole Genome 55 K Bioarray (GE Healthcare, Buckinghamshire, UK) and the hybridization signal was normalized by using CodeLink System Software Analysis (GE Healthcare). The differentially expressed genes were selected based on the Student *t*-test considering a *P*-value<0.01 as significant. Gene ontology analysis was performed by using the ToppGene suite (http://toppgene.cchmc.org).

Real time RT-PCR analysis

To confirm the gene expression evaluated by cDNA microarray, real time RT-PCR analysis was performed for some selected genes. Gene-specific primers were designed by using primer 3 software (http://frodo.wi.mit.edu/primer3/) to generate a PCR product in the 3′ portion, spanning the translated region of the target mRNA. RT was performed with 0.5 μg/μl oligo(dT)1-18 primers (Invitrogen), 10 nM dNTPs and SupersScrit III (Invitrogen, Santa Clara, Calif., USA). cDNA samples (6 μl at 20 ng/μl) were subjected to quantitative PCR assays in duplicate by using SYBR Green methodology in a Rotor-Gene 6 System and the respective software (Cobertt Research, Mortlake, Australia). BLAST (basic local alignment search tool; blast.ncbi.nlm.nih.gov) analysis was carried out to confirm specificity. Reaction conditions were: 95°C for 15 min, followed by 40 cycles at 95°C for 15 s and 60°C for 1 min. Results displaying a CT variation between them of <1.0 were further used to calculate average values. *GAPDH* (D-glyceraldehyde-3-phosphate dehydrogenase) was used as an internal control, with the HB4A normal mammary cell line (for samples that were HER2-negative) or C5.4 (HB4A cell line transfected with HER2, for tumor samples with HER2 overexpression) as a reference sample. Relative gene expression of target genes was calculated by using the $2^{-\Delta\Delta Ct}$ method.

Co-expression network

For the construction of networks, we used the genes differentially expressed after rapamycin treatment of breast cancer slices and respective controls. HER2-positive and HER2-negative groups were analyzed separately. Using the expression values of the microarray, we calculated the Pearson Correlation Coefficient (PCC) between pairs of genes independently for controls or treated samples (Taylor et al. 2009). Differences between the correlations displayed by either controls or treated groups were ranked for gene pairs. Pairs with absolute differences greater than 1.0 were selected. The aim was to select pairs of genes that had changed their co-expression between the control and rapamycin-treated slices. Data analysis and visualization were conducted by Cytoscape software (version 2.8.0; www.cytoscape.org).

Results

Our first step was to assess the morphological integrity of breast cancer slices submitted to culture conditions. Control samples, cultured in the absence of rapamycin for 24 h (C), were morphologically well preserved, as compared with samples not submitted to culture conditions (T0). We had previously shown, through BrdU uptake, that the proliferative capacity of tumor slices was approximately 10% (Milani et al. 2010). In accordance, under similar conditions, our data indicate that tumor slice viability was preserved in culture conditions for 24 h.

Table 1 Phosphoprotein expression in breast cancer samples. Tumor expression was considered positive for specific phosphoprotein if at least 10% of tumor cells (≥1+) were stained and was considered moderate/intense if more than 20% of tumor cells (2+/3+) were stained. Reduction in phosphoprotein abundance (*RPA*) reflects the percentage of tumor samples presenting a decreased number of stained cells (evaluated as 0/1+/2+/3+) after rapamycin exposure (*p* phosphorylated, *AKT* protein kinase B, *mTOR* mammalian target of rapamycin, *S6K1* p70 ribosomal protein S6 kinase, *4EBP1* eukaryotic initiation factor 4E-binding protein 1)

Tumor expression level	p-AKT(threo)	p-mTOR	p-S6K1	p-4EBP1
≥10% cells (≥1+)	27/30 (90.0)	26/30 (86.7%)	25/30 (83.3%)	30/30 (100.0%)
>20% cells (2+/3+)	13/30 (43.3%)	18/30 (60.0%)	19/30 (63.3%)	28/30 (93.3%)
RPA	8/30 (26.7%)	8/30 (26.7%)	7/30 (23.3%)	18/30 (60.0%)

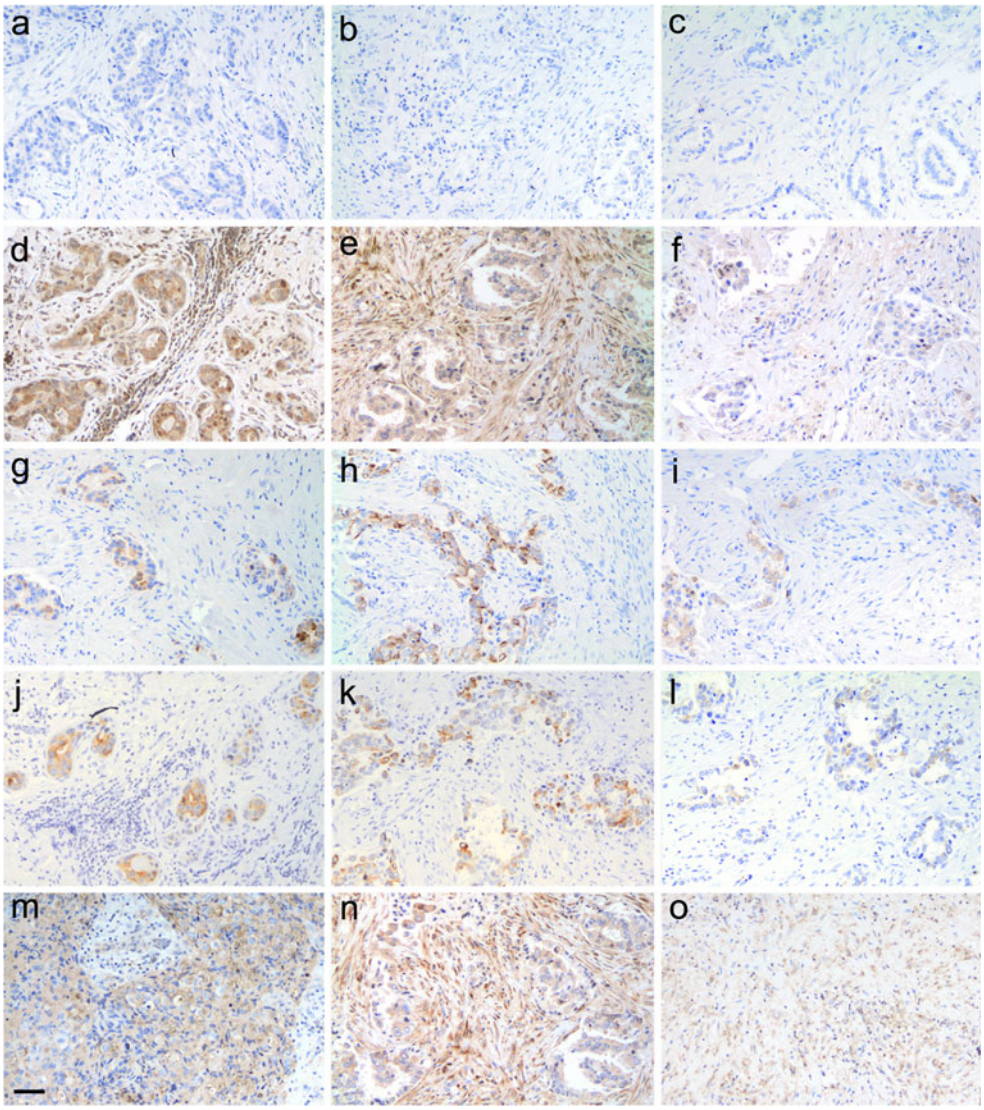

Fig. 1 Representative immunohistochemical staining of negative controls, i.e., primary antibody absent (**a–c**), p-AKT (phosphorylated protein kinase B; **d–f**), p-mTOR (phosphorylated mammalian target of rapamycin; **g–i**), p-4EBP1 (phosphorylated eukaryotic initiation factor 4E-binding protein 1; **j–l**) and p-S6K1 (phosphorylated p70 ribosomal protein S6 kinase; **m–o**) in slices of ductal breast carcinoma before culture (T0; **a**, **d**, **g**, **j**, **m**) and maintained in culture without (**b**, **e**, **h**, **k**, **n**) or with (**c**, **f**, **i**, **l**, **o**) rapamycin (20 nM) for 24 h. *Bar* 100 μm

Next, we evaluated the AKT/mTOR pathway activation through the expression of the phosphorylated forms of AKT, mTOR and the downstream intermediates 4EBP1 and S6K1, considering as positive samples those with at least 10% stained tumor cells. In untreated tumor slices, the phosphorylated forms of the proteins were detected in the majority of the samples (Table 1). In addition, phosphoprotein expression considered as moderate/intense in tumors with more than 20% positive cells was detected in at least 43.3% of the tumor samples not exposed to rapamycin. Cultured tissue slices retained their ability to express members of the p-AKT pathway compared with the corresponding initial time (T0; see Supplementary Table S1).

After rapamycin treatment (24 h), a trend was noted towards the reduced activity of the pAKT/mTOR pathway, as the proportion of positive tumor cells for the phosphorylated forms of AKT, mTOR, S6K1 and 4EBP1 decreased in 26.7%, 26.7%, 23.3% and 60.0 % of the cases, respectively (Table 1). Examples of immunohistochemical staining of p-AKT, p-

Table 2 Proportion of tumors presenting phosphoprotein reduction following rapamycin exposure, according to *HER2* (epidermal growth factor receptor-type 2) and *ER* (estrogen receptor) expression. Twelve tumors presented HER2 overexpression and were considered HER2-positive (*HER2-pos*) in contrast with 18 considered as HER2-negative (*HER2-neg*). Eighteen tumors expressed ER (*ER-pos*) and 12 did not (*ER-neg*). Reduction in phosphoprotein abundance reflects the percentage of tumor samples presenting a decreased number of stained cells (evaluated as 0/1+/2+/3+) after rapamycin exposure. Number of samples with reduced phosphoprotein expression after rapamycin exposure and percentages are shown

Expression	p-AKT(threo)	p-mTOR	p-S6K1	p-4EBP1
HER2-neg (*n*=18)	3 (16.7%)	5 (27.8%)	5 (27.8%)	9 (50.0%)
HER2-pos (*n*=12)	5 (41.7%)	3 (25.0%)	2 (16.7%)	9 (75.0%)
ER-neg (*n*=12)	3 (25.0%)	1 (8.3%)	3 (25.0%)	8 (66.7%)
ER-pos (*n*=18)	5 (27.8%)	7 (38.9%)	4 (22.2%)	10 (55.6%)

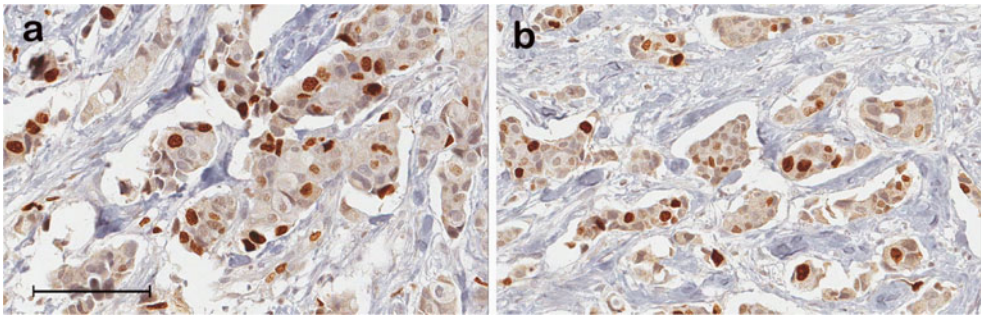

Fig. 2 Representative immunohistochemical staining of Ki67 in slices of ductal breast carcinoma maintained in culture without (**a**) and with (**b**) rapamycin (20 nM) for 24 h. *Bar* 100 μm

mTOR, p-4EBP1 and p-S6K1 in slice samples before culture (T0) and maintained in the absence or presence of rapamycin are shown in Fig. 1 (see also Supplementary Tables S1, S2). A significant change in phosphoprotein expression was not detected in HER2-positive compared with HER2-negative samples or in ER-negative versus ER-positive cases (Table 2). Positive expression of the proliferation marker Ki67 (≥10%) was detected in 68% of the cases. The median Ki67 percentage was 25% (range: 10%–80%). A representative example of nuclear Ki67 staining is displayed in Fig. 2. No significant change was observed in Ki67 expression between pre- and post-treatment samples.

We then sought to evaluate rapamycin effects on the gene expression profile of breast cancer samples, by using microarrays. For this analysis, 10 paired tumor samples (cultured with or without rapamycin) were divided into two groups, according to the expression of HER2 (absent or overexpressed), since one of the major signaling pathways utilized by HER2 is reported to be the PI3K/AKT pathway (Zhou et al. 2004; Park and Kim 2007; Tokunaga et al. 2006). All ten samples chosen for microarray analyses, namely the five HER-positive and five HER-negative samples, displayed different phosphorylation levels of p-AKT, p-mTOR and p-S6K1 but only one case (HER-negative) did not display p-4EBP1 downregulation upon

Table 3 Ontological biological functions of differentially expressed genes from HER2-negative tumors following rapamycin treatment (↑ upregulated, ↓ downregulated)

Function	Genes
Regulation of canonical Wnt receptor signaling pathway	SMAD3↑ LRP6↑ SHH↑
Ubiquitin-dependent protein catabolic process	USP29↑ SHH↑ HSP90B1↓ USP10↓
Intracellular transport	SLC25A13↓ KPNA2↓ SMAD3↑ LRP6↑ SFRS9↓ EXPH5↑ NUP133 ↓ SHH↑ SNAPAP↓
Protein phosphorylation	CAMK2D↑ PAK6↑ MAPK9↓ SMAD3↑ LRP6↑ TP53RK↓ OBSCN↑ ACVR2A↑ OXSR1↓
Response to hypoxia	CAMK2D↑ SMAD3↑ SHH↑ HSP90B1↓
Nuclear transport	KPNA2↓ SMAD3↑ SFRS9↓ NUP133 ↓ SHH↑
Apoptosis	API5↓ RNF130↑ MAPK9↓ SMAD3↑ LRP6↑ OBSCN↑ SHH↑ HSP90B1↓
RNA splicing via transesterification reactions	MBNL1↑ SFRS9↓ RBM17↓ PRPF3↓
RNA transport	SFRS9↓ NUP133↓ CKAP5↓
Organic substance transport	SLC27A3↑ SLC25A13↓ MAPK9↓ SLC44A1↓ LRP6↑ NUP133↓
Positive regulation of transmembrane transport	SMAD3↑ SHH↑
Protein transport	KPNA2↓ SMAD3↑ TOMM40L↑ EXPH5↑ NUP133↓ SHH↑ HSP90B1↓ SNAPAP↓
Positive regulation of transport	MAPK9↓ SMAD3↑ ACVR2A↑ SHH↑
Nuclear import	KPNA2↓ SMAD3↑ SHH↑
Intracellular protein transport	KPNA2↓ SMAD3↑ EXPH5↑ SHH↑ SNAPAP↓
Lipid transport	SLC27A3↑ MAPK9↓ LRP6↓
Fatty acid transport	SLC27A3↑ MAPK9↓
Translation	MRPS30↓ MRPL37↓ TSFM↓
Macromolecule catabolic process	HSP90B1↓ KIAA1008↓ USP29↑ SHH↑ USP10↓
Regulation of catalytic activity	MAPK9↓ SMAD3↑ IQGAP1↑ LRP6↑ EXPH5↑ OBSCN↑ KIAA1008↓ ACVR2A↑ HSP90B1↓
Negative regulation of protein metabolic process	SMAD3↑ MBNL1↑ LRP6↑ ACVR2A ↑ HOXB5↑ NUP133↓ SHH↑

rapamycin treatment. The inhibition of 4EBP1 phosphorylation in response to treatment of the different tumors was variable (see Supplementary Table S2). Since the tissues might be heterogeneous regarding the composition of various cell types, we evaluated, in nine from those ten paired tumor samples, the percentages of malignant epithelial, stromal and immune cells (see Supplementary Table S3). We observed that the median percentage of the malignant cells in the control samples was 67% (range: 61%–75%), whereas after rapamycin treatment, the median was maintained (67%), although the range varied from 27% to 77%. In stromal cells, the median frequency was 26% (range: 11%–45%) in control samples and after rapamycin treatment, the frequency ranged from 13% to 64% (median: 24%). The inflammatory cell infiltrate was mild, ranging from 2% to 20% for controls cells (median: 11%), whereas in the rapamycin-treated slices, immune cell frequency ranged from 4% to 17% (median: 10%).

In HER2-overexpressing samples, drug-induced changes were detected in 48 transcripts ($P<0.01$), most of which (83%) were downregulated by the treatment. In HER2-negative tumors, 56 genes were differentially expressed, among which 57% were downregulated (see Supplementary Tables S4 and S5). No genes were commonly regulated in both tumor groups defined by the overexpression or absence of HER2, emphasizing the variability in gene expression changes induced by rapamycin in the different cellular contexts. Differentially expressed genes were sorted by gene ontology (biological function; Tables 3, 4) and the majority of genes differentially expressed in HER2-negative tumors after rapamycin treatment mapped to the following biological processes: "negative regulation of Wnt receptor signaling pathway", "ubiquitin-dependent protein catabolic process", "apoptosis", "protein transport" and "phosphorylation" (Table 3). In HER2-overexpressed samples, differentially expressed genes were associated with "cell proliferation", "response to hormone stimulus", "positive and negative regulation of gene expression", "carbohydrate biosynthetic process", "amine metabolic process", "steroid metabolic process" and "transmembrane transport" (Table 4). Most genes included in these functions were downregulated by rapamycin.

Some genes were selected for further analysis by quantitative RT-PCR. Twenty paired tumor samples (cultured with or without rapamycin) were analyzed, of which 10 were HER-positive and 10 HER-negative. Three patients, namely one HER-positive (patient 31) and two HER-negative (patients 32 and 33), were further included only for real-time

Table 4 Ontological biological functions of differentially expressed genes from HER2-positive tumors following rapamycin treatment (↑ upregulated, ↓ downregulated)

Function	Genes
Cell proliferation	TGM2↓ SCARB1↓ NOLC1↓ ITGB1↓ THRB↓ TCF2↓ PRKCQ↓ ZMYND11↓ CHRM1↓ DACH1↑ GATA4↓ IL7R↓ MXD4↓ NR3C2 ↓ IL11RA↓
Transcription from RNA polymerase II promoter	TFEB↓ MTF1↓ THRB↓ TCF2↓ ZMYND11↓ DACH1↑ GATA4↓ MXD4↓ KLF7↓ NR3C2↓
Response to hormone stimulus	EIF4B↓ PAM↓ THRB↓ PPAT↓ PRKCQ↓ GATA4↓ NR3C2↓
Glycosaminoglycan biosynthetic process	EXT1↓ GCNT2↑
Positive regulation of macromolecule biosynthetic process	TFEB↓ NOLC1↓ MTF1↑ THRB↓ TCF2↓ PRKCQ↓ GATA4↓ KLF7↓
Regulation of gene-specific transcription	TFEB↓ THRB↓ TCF2↓ GATA4↓ NR3C2↓
Positive regulation of transcription, DNA-dependent	TFEB↓ MTF1↑ THRB↓ TCF2↓ GATA4↓ KLF7↓
Positive regulation of cellular metabolic process	TFEB↓ NOLC1↓ MTF1↑ ITGB1↓ THRB↓ TCF2↓ PRKCQ↓ GATA4↓ KLF7↓
Response to steroid hormone stimulus	PAM↓ THRB↓ GATA4↓ NR3C2↓
Positive regulation of gene expression	TFEB↓ NOLC1↓ MTF1↑ THRB↓ TCF2↓ GATA4↓ KLF7↓
Positive regulation of nucleobase, nucleoside, nucleotide and nucleic acid metabolic process	TFEB↓ NOLC1↓ MTF1↑ THRB↓ TCF2↓ GATA4↓ KLF7↓
Carbohydrate biosynthetic process	EXT1↓ GCNT2↑ PC↓ DPM1↑
Amine metabolic process	EXT1↓ ASS↑ COLQ↓ PPAT↓ GCNT2↑
Transmembrane transport	ABCD4↓ SCARB1↓ SLC23A1↓ NOLC1↓ FLJ10847↑ PRKCQ↓ ABCC10↓
Negative regulation of transcription	THRB↓ TCF2↓ Z MYND11↓ DACH1↑ MXD4↓
Regulation of intracellular protein transport	NOLC1↓ PRKCQ↓
Steroid metabolic process	SCARB1↓ THRB↓ WWOX↓
Negative regulation of gene expression	THRB↓ TCF2↓ ZMYND11↓ DACH1↑ MXD4↓
Negative regulation of macromolecule biosynthetic process	THRB↓ TCF2↓ ZMYND11↓ DACH1↑ MXD4↓
Glutamine metabolic process	PPAT↓

RT-PCR analysis. Because of the low levels of the total RNA extracted from slice samples, we evaluated at least six paired tumor samples for each gene.

In microarray experiments, the selected genes were found to be regulated following rapamycin exposure. In HER2-negative samples, three of them were considered less expressed, namely *MRPS30* and *MRPL37* (related to translation) and *GTF2E2* (a transcription factor), while in HER2-overexpressing samples, three of them were related to metabolic processes, namely *EXT1* and *WWOX* (less expressed) and *DPM1* (more expressed) and another gene, *IL11RA*, was related to cell proliferation (less expressed). Another two transcripts were analyzed in HER2-positive (overexpression) samples, namely *PHGDH* (phosphoglycerate dehydrogenase) mRNA, which codes for an enzyme that catalyses the first step in the serine biosynthesis pathway (Possemato et al. 2011) and which was found to be regulated by rapamycin in breast cancer cell lines in our previous work (Trapé et al. 2012) and *ATG6*/*BECN1* mRNA, which codes for beclin-1 and which is involved in autophagy (Pattingre et al. 2008), a process that might be regulated by rapamycin.

In HER2-negative samples, both *MRPS30* and *MRPL37* were statistically confirmed as being less expressed after rapamycin treatment, whereas the downregulation of GTF2E2 was observed in only 60% of the cases (Fig. 3). In HER2-positive tumors, no statistical changes in *EXT1*, *WWOX*, *DMP1*, or *ATG6* levels after rapamycin treatment were detected; however, a trend was seen towards the downregulation of *IL11RA*, *DMP1* and *PHGDH* (Fig. 4).

Using the set of genes differentially expressed between slices after treatment with rapamycin and the respective untreated controls, we next constructed gene-gene co-expression networks by using the Pearson correlation between pairs of genes differentially expressed in each group (HER2-positive or -negative). Differences between the correlations in each group were ranked for gene pairs and those with high absolute differences indicated that the two correlations were on the opposite sides of zero and closer to 1 and −1 or vice-versa. By restricting the analysis to those with absolute differences greater than 1.0, we selected groups of 21 and 32 gene pairs, respectively, in HER2-positive and HER2-negative subsets (see Supplementary Tables S6 and S7). Figures 5, 6 show the changes in the correlation of the co-expression of gene pairs before and after rapamycin addition in both groups. Notably, we found, in each group, pairs of genes in which correlation coefficients in controls were inverted after rapamycin treatment. Our network analysis suggested rapamycin participation in degradative processes and transforming growth factor-β1 (TGFβ1) signaling.

Discussion

The major focus of the present study has been to examine the reliability of an ex-vivo organotypic culture of human breast carcinoma as a model to evaluate differential rapamycin effects in terms of gene expression in tumors

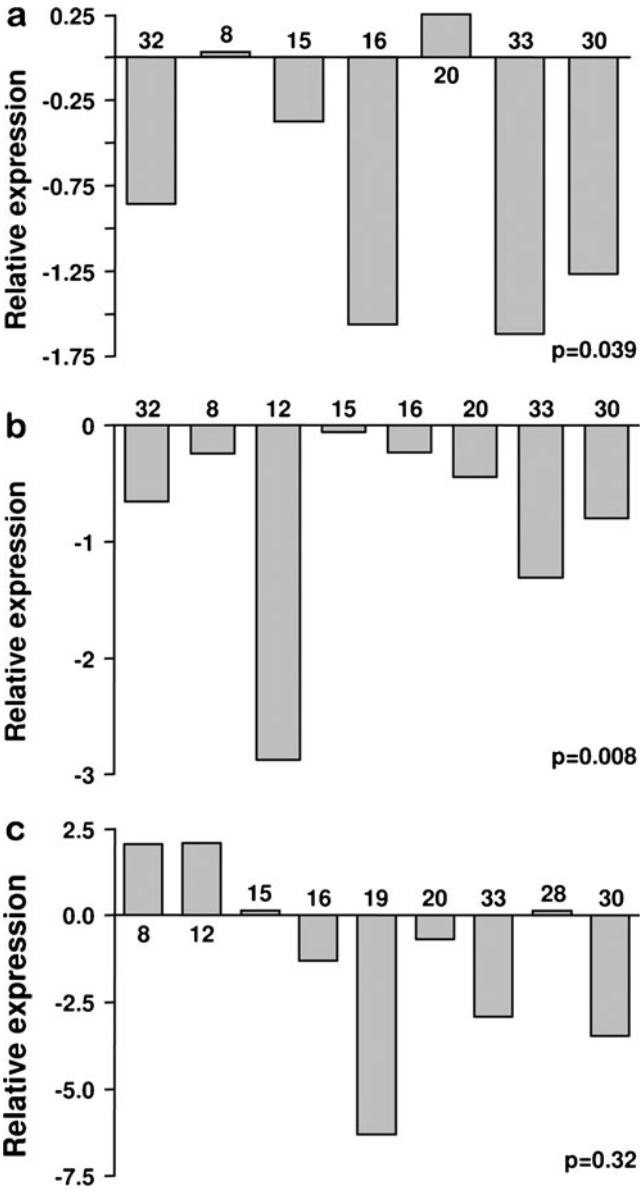

Fig. 3 Expression of *MRPS30* (**a**), *MRPL37* (**b**) and *GTF2E2* (**c**) in breast cancer samples, categorized as being epidermal growth factor receptor-type 2 (HER2)-negative, treated with rapamycin. Breast cancer slices were cultured in the presence or absence of rapamycin (20 nM) for 24 h and gene expression was evaluated by reverse transcription with quantitative polymerase chain reaction (RT-qPCR). Relative expression of target genes in rapamycin-treated samples was calculated by using the $2^{-\Delta\Delta Ct}$ method with *GAPDH* (D-glyceraldehyde-3-phosphate dehydrogenase) as an internal control and corresponding untreated samples as a reference. Expression values were log2-transformed and are shown on the *y-axis* for each individual sample (specified on the *x-axis*). *P*-values were obtained by a paired *t*-test

overexpressing or negative for HER2. Gene expression profiles have classified breast cancer into subtypes, each one reflecting their different biology and different outcomes (Sørlie et al. 2001) and therefore biological markers that define the response to rapamycin should vary among the various breast cancer subtypes (Hernandez-Aya and Gonzalez-Angulo 2011). Previous studies have emphasized a correlation between the activated AKT signaling pathway and HER2 overexpression (Yu et al. 2001; Zhou et al. 2004; Park and Kim 2007).

The concentration of rapamycin (20 nM) used in this study was chosen based on pharmacokinetic studies of everolimus, which is a rapamycin analog that has the same mechanism of action (Raymond et al. 2004; Tabernero et al. 2008; O'Reilly and McSheehy 2010). Based on the safety profile of everolimus, Tabernero et al. (2008) defined that satisfactory mTOR signaling inhibition occurred at daily doses of 10 mg, which lead to a steady-state serum concentration of 21.4 ng/ml (23 nM). Maximum and trough concentrations are 67 nM and 18 nM, respectively, with an approximate half-life of 38 h. In addition, in 48 different mammalian cell lines treated with everolimus, an IC50 at ≤65nM was detected in 70% and an IC50 between 1-10nM in 50% of the lineages (O'Reilly and McSheehy 2010).

We have investigated the incidence of AKT/mTOR activation in our samples. Our results show that the phosphorylated forms of AKT, mTOR, S6K1 and 4EBP1 are detectable in the majority of tumor samples cultured in the absence of rapamycin in a similar range reported by previous authors (Zhou et al. 2004; Andre et al. 2008; Rojo et al. 2007; Bose et al. 2006), indicating that the AKT pathway is active in most of our breast cancer samples. In addition, our results confirm a positive association between the p-AKT and p-4EBP1 frequency of expression and large tumor size (Rojo et al. 2007; Vestey et al. 2005).

After rapamycin treatment, we discerned a trend towards the reduced activity of the pAKT/mTOR pathway, detected as a decreased proportion of tumor cells expressing the phosphoproteins. A hyperactivation of AKT by rapamycin treatment as suggested by O'Reilly et al. (2006) with consequent phosphorylation at Thr308 was not observed in our cases. However, an increment of p-AKT by rapamycin was reported previously to occur in only 60% of tumors from treated patients (Tabernero et al. 2008). Of particular interest was the expression of p-4EBP1, which was reduced in 60% of the cases after rapamycin treatment, since p-4EBP1 has eight described phosphorylation sites, the majority being decreased by rapamycin. However, in our cases, 4EBP1 phosphorylation

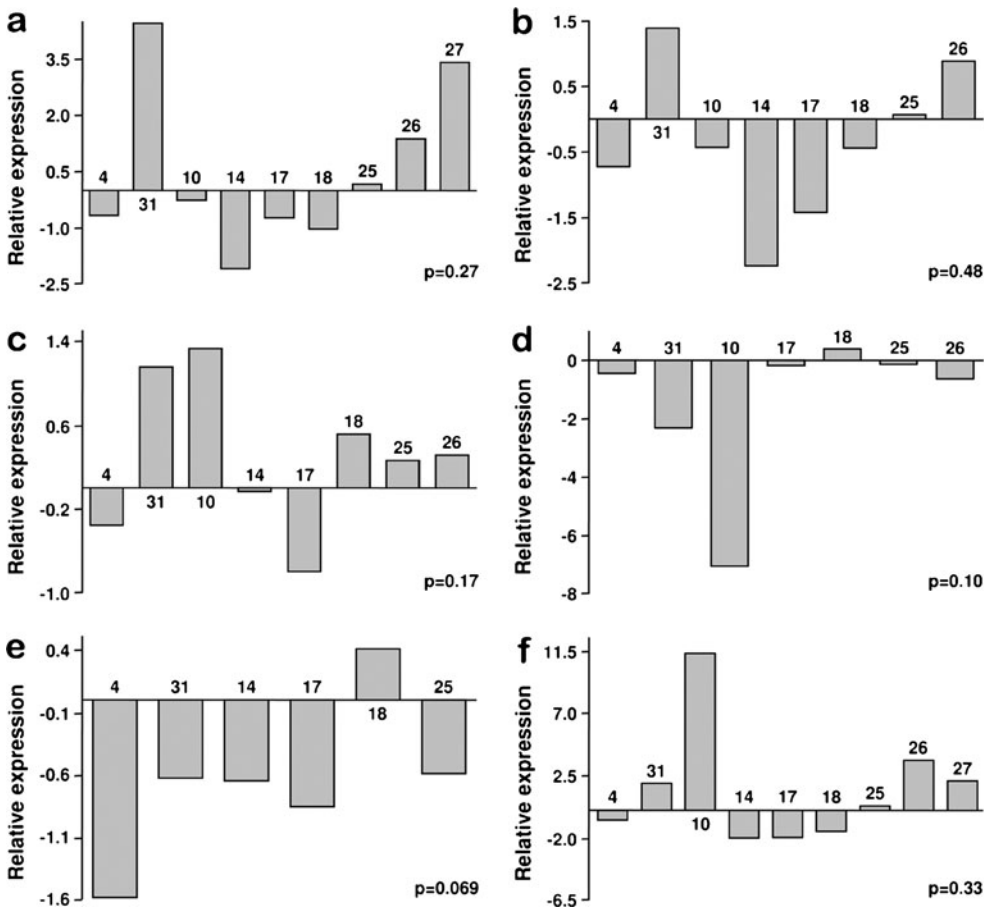

Fig. 4 Expression of *EXT1* (**a**), *WWOX* (**b**), *DPM1* (**c**), *IL11RA* (**d**), *PHDGH* (**e**) and *ATG6* (**f**) in breast cancer samples with HER2 overexpression, treated with rapamycin. Breast cancer slices were cultured in the presence or absence of rapamycin (20 nM) for 24 h and gene expression was evaluated by RT-qPCR. Relative expression of target genes in rapamycin-treated samples was calculated by using the $2^{-\Delta\Delta Ct}$ method with *GAPDH* as an internal control and corresponding untreated samples as a reference. Expression values were log2-transformed and are shown on the *y-axis* for each individual sample (specified on the *x-axis*). *P*-values were obtained by a paired *t*-test

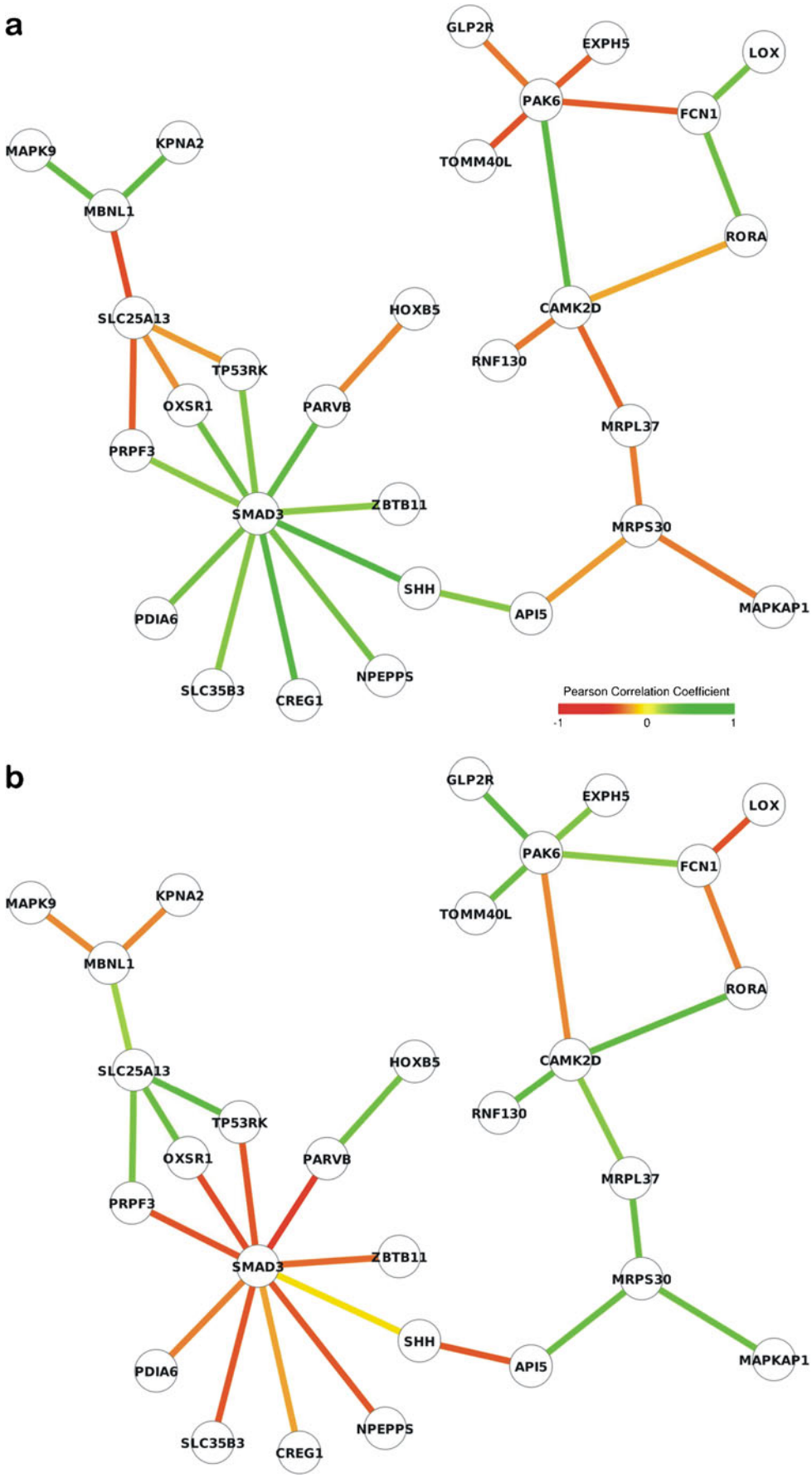

Fig. 5 Networks indicating connections between pairs of genes in which the links representing Pearson correlation coefficients show gene expression differences higher than 1.0 for the HER2-negative group before and after rapamycin treatment. Links in the HER2-negative controls (**a**) and links after rapamycin treatment (**b**)

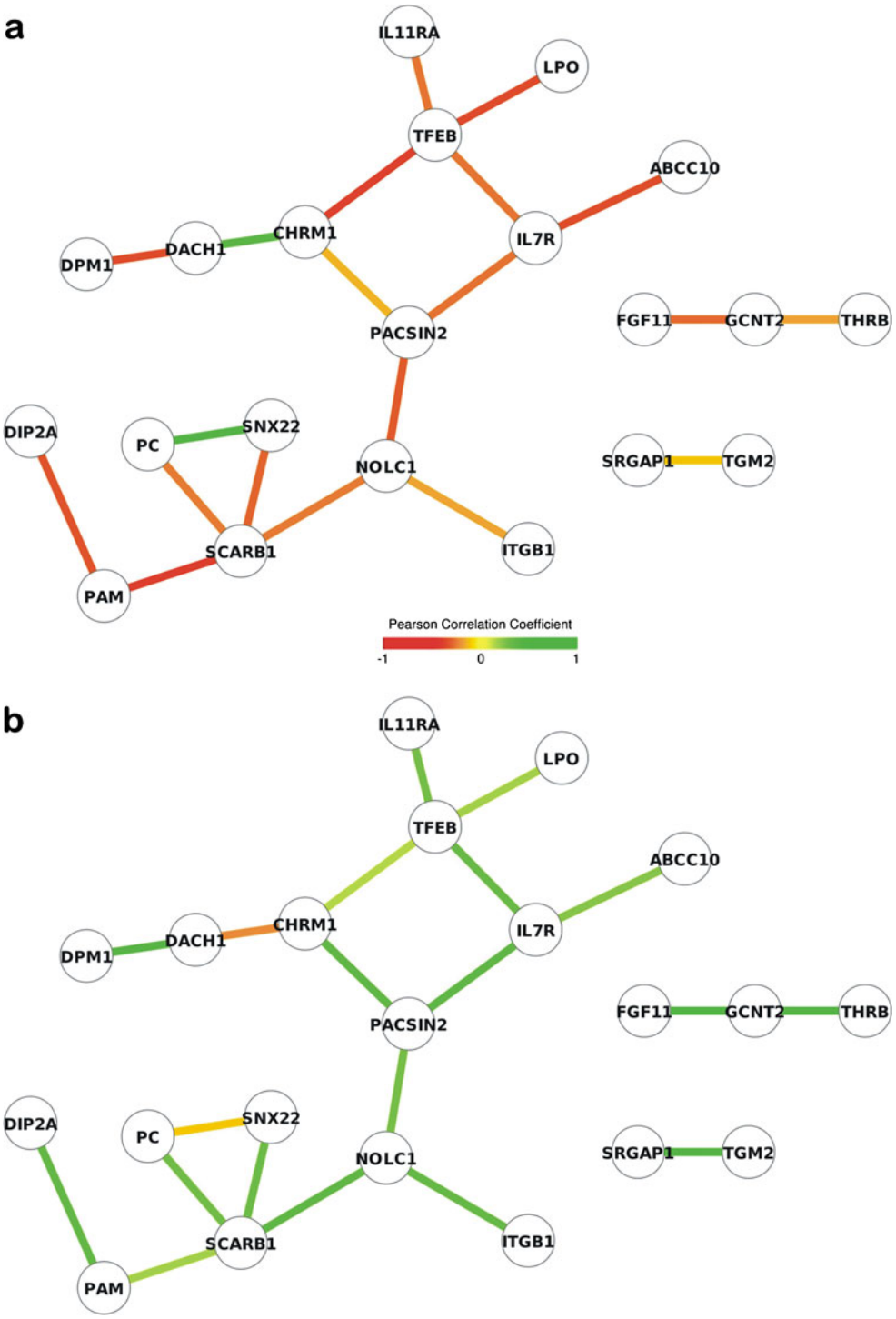

Fig. 6 Networks indicating connections between pairs of genes in which the links representing Pearson correlation coefficients show gene expression differences higher than 1.0 for the HER2-positive group before and after rapamycin treatment. Links in the HER2-positive controls (**a**) and links after rapamycin treatment (**b**)

was not associated with changes in the tumor proliferative index evaluated through Ki67 expression. Our results are in accordance with previous work employing cell lines and tumor biopsies showing that the reduction in p-4EBP1 expression is probably unrelated to sensitivity to rapamycin (Noh et al. 2004; Satheesha et al. 2011). We have previously observed dephosphorylation of p-4EBP1 with no changes in cell cycle distribution in a HER2-positive breast cancer lineage after a short (24 h) rapamycin treatment (Trapé et al. 2012). Thus, reduced Ki67 tumor expression might become apparent only after a long-term treatment, as previously described (Macaskill et al. 2011; Sabine et al. 2010; Tabernero et al. 2008).

Among the genes downregulated by rapamycin in HER2-positive tumors, several are involved in cell proliferation and amino-acid metabolic processes suggesting an inhibition of biosynthetic pathways. For example, in accordance with our

previous results in an HER2-positive cell line, *PHGDH*, which is involved in L-serine and consequently amino-acid synthesis specifically regulated by the HER2 oncogene (Bollig-Fischer et al. 2011), is downregulated by rapamycin (Possemato et al. 2011; Trapé et al. 2012). Previous reports have suggested that genes associated with protein/amino-acid dephosphorylation and proliferation or encoding enzymes of the glycolysis pathway are downregulated by rapamycin analogs (Sabine et al. 2010; Majumder et al. 2004).

In HER2-negative tumors, rapamycin inhibits translation at many levels by repressing mitochondrial ribosomal protein synthesis (*MRPS30*, *MRPL37*) and the translational elongation mitochondrial factor (*TSFM*). In accordance, mitochondrial dysfunction leading to the inhibition of mTOR has been previously reported (Desai et al. 2002). Other altered genes in this set are involved in diverse cellular functions, such as transport, the synthesis or use of amino-acids and lipid metabolism.

Network-based analyses can implicate genes with apparently low discriminate potential, if such genes participate in functional modules (Chuang et al. 2007). Most cellular functions are understood as being carried out by groups of molecules within functional modules (Barabási and Oltvai 2004). Thus, to explore further the relevance of these two sets of genes classified in HER2-positive or HER2-negative cells, we aimed to identify gene pairs with differential co-expression patterns in two cellular states (before and after rapamycin treatment). Our network analysis demonstrated a disruption of co-expression between several pairs of genes in response to rapamycin treatment. In one example, in HER2-positive cells, we noted that the transcription factor EB (*TFEB*), which is one of the hubs (highly connected nodes), is linked to each one of the receptors *IL7R*, *IL11RA* and *CHRM1* and to lactoperoxidase (*LPO*). They show negative co-regulation at the control stage and positive correlation after rapamycin treatment. Under full nutrients, mTORC-1 phosphorylates TFEB (a master regulator of lysosomal biogenesis; Peña-Llopis et al. 2011) and inhibits TFEB activity. Conversely, the inhibition of mTORC-1 leads to the translocation of TFEB to the nucleus where it activates transcriptional response to autophagic genes that might contribute to membrane receptor endocytosis (Settembre et al. 2012), suggesting an impact with regard to this different co-expression between treated and control tumors.

In HER2-negative cases, we have noted the positive co-expression of *SMAD3* (a protein of the TGFβ signaling axis) and several co-interacting genes. One of these genes is sonic hedgehog (*SHH*), which activates the hedgehog signaling pathway, which in turn enhances cellular motility and invasion and this occurs through the TGFβ signaling *SMAD3* (mothers against DPP homolog 3; Yoo et al. 2008). Other partners of *SMAD3* included *CREG* (inhibitor of apoptosis; Deng et al. 2010), *OXSR1* (oxidative stress response), *PARVB* (implicated in motility, growth and survival) and NPEPPS (aminopeptidase puromycin sensitive protein; PSA, prostate-specific antigen). Rapamycin treatment decreases correlations between SMAD3 and its partners, possibly attenuating their effects.

One limitation of the present study is that the number of patients analyzed herein is too small to allow a definitive conclusion to be drawn. Our present observation thus needs to be confirmed by a future study covering a larger number of samples.

In summary, our results suggest that the ex-vivo culture method preserves AKT/mTOR pathway activity. In addition, we have found that several genes associated with biosynthetic and catabolic process are modulated by rapamycin treatment, as suggested in previous studies (Peng et al. 2002; Majumder et al. 2004). The co-expression network approach has indicated several pairs of genes that change their interactions levels after rapamycin treatment. Therefore, this strategy based on the organotypic short-term culture of breast cancer samples might provide an in vitro setting for molecular studies of the biological effects of rapamycin treatment on individual breast cancer samples.

Acknowledgments We are indebted to Dr. C. Krumdieck (University of Alabama, Birmingham, Ala., USA) for the kind donation of the Krumdieck tissue slicer to our institution. We also thank Dr. Igor Moyses Longo Snitcovsky for critical suggestions, Dr. Fiorita G. L. Mundim for helping with the immunohistochemical determinations, Mrs. Maria Jose Gonçalves Benevides for secretarial help and Mrs. Cristina Piñeiro Grandal for figure edition.

S.H.G.G. provided the tumor samples, prepared the tissue slices, collected all clinical data and was involved in drafting the manuscript. M.L.H.K. performed the culture, microarray and RT-PCR experiments. R.A.R. performed the microarray determinations. H.B. and R.A.R. performed the microarray data analysis. S.N., F.A.S. and A.F.L.W. participated in the immunohistochemistry studies. L.L. carried out the analysis of the co-expression network. J.C.S.G. provided clinical support for patient recruitment. M.A.A.K.F., M.L.H.K. and F.S.P. carried out the statistical analysis. M.M.B. was responsible for the study conception. M.M.B. and M.A.A.K.F. were involved in study design and manuscript preparation.

References

Akcakanat A, Zhang L, Tsavachidis S, Meric-Bernstam F (2009) The rapamycin-regulated gene expression signature determines prognosis for breast cancer. Mol Cancer 8:75

Andre F, Nahta R, Conforti R, Boulet T, Aziz M, Yuan LX et al (2008) Expression patterns and predictive value of phosphorylated AKT in early-stage breast cancer. Ann Oncol 19:315–320

Barabási AL, Oltvai ZN (2004) Network biology: understanding the cell's functional organization. Nat Rev Genet 5:101–113

Barbosa EM, Nonogaki S, Katayama ML, Folgueira MA, Alves VF, Brentani MM (2004) Vitamin D3 modulation of plasminogen activator inhibitor type-1 in human breast carcinomas under organ culture. Virchows Arch 444:175–182

Bläuer M, Tammela TL, Ylikomi T (2008) A novel tissue-slice culture model for non-malignant human prostate. Cell Tissue Res 332:489–498

Bollig-Fischer A, Dewey TG, Ethier SP (2011) Oncogene activation induces metabolic transformation resulting in insulin-independence in human breast cancer cells. PLoS One 6:e17959

Bose S, Chandran S, Mirocha JM, Bose N (2006) The Akt pathway in human breast cancer: a tissue-array-based analysis. Mod Pathol 19:238–245

Chuang HY, Lee E, Liu YT, Lee D, Ideker T (2007) Network-based classification of breast cancer metastasis. Mol Syst Biol 3:140

Deng J, Han Y, Yan C, Tian X, Tao J, Kang J, Li S (2010) Overexpressing cellular repressor of E1A-stimulated genes protects mesenchymal stem cells against hypoxia- and serum deprivation-induced apoptosis by activation of PI3K/Akt. Apoptosis 15:463–473

Desai BN, Myers BR, Schreiber SL (2002) FKBP12-rapamycin-associated protein associates with mitochondria and senses osmotic stress via mitochondrial dysfunction. Proc Natl Acad Sci USA 99:4319–4324

Dillon RL, White DE, Muller WJ (2007) The phosphatidyl inositol 3-kinase signaling network: implications for human breast cancer. Oncogene 26:1338–1345

Dudkin L, Dilling MB, Cheshire PJ, Harwood FC, Hollingshead M, Arbuck SG, Travis R, Sausville EA, Houghton PJ (2001) Biochemical correlates of mTOR inhibition by the rapamycin ester CCI-779 and tumor growth inhibition. Clin Cancer Res 7:1758–1764

Finak G, Bertos N, Pepin F, Sadekova S, Souleimanova M, Zhao H, Chen H, Omeroglu G, Meterissian S, Omeroglu A, Hallett M, Park M (2008) Stromal gene expression predicts clinical outcome in breast cancer. Nat Med 14:518–527

Guertin DA, Sabatini DM (2007) Defining the role of mTOR in cancer. Cancer Cell 12:9–22

Heinonen H, Nieminen A, Saarela M, Kallioniemi A, Klefström J, Hautaniemi S et al (2008) Deciphering downstream gene targets of PI3K/mTOR/p70S6K pathway in breast cancer. BMC Genomics 9:348

Hernandez-Aya LF, Gonzalez-Angulo AM (2011) Targeting the phosphatidylinositol 3-kinase signaling pathway in breast cancer. Oncologist 16:(4)404–414

Macaskill EJ, Bartlett JM, Sabine VS, Faratian D, Renshaw L, White S, Campbell FM, Young O, Williams L, Thomas JS, Barber MD, Dixon JM (2011) The mammalian target of rapamycin inhibitor everolimus (RAD001) in early breast cancer: results of a pre-operative study. Breast Cancer Res Treat 128:725–734

Majumder PK, Febbo PG, Bikoff R, Berger R, Xue Q, McMahon LM et al (2004) mTOR inhibition reverses Akt-dependent prostate intraepithelial neoplasia through regulation of apoptotic and HIF-1-dependent pathways. Nat Med 10:594–601

Meric-Bernstam F, Gonzalez-Angulo AM (2009) Targeting the mTOR signaling network for cancer therapy. J Clin Oncol 27:2278–2287

Milani C, Welsh J, Katayama ML, Lyra EC, Maciel MS, Brentani MM, Folgueira MA (2010) Human breast tumor slices: a model for identification of vitamin D regulated genes in the tumor microenvironment. J Steroid Biochem Mol Biol 21:151–155

Mira-y-Lopez R, Osborne MP, DePalo AJ, Ossowski L (1991) Estradiol modulation of plasminogen activator production in organ cultures of human breast carcinomas: correlation with clinical outcome of anti-estrogen therapy. Int J Cancer 47:827–832

Noh WC, Mondesire WH, Peng J, Jian W, Zhang H, Dong J et al (2004) Determinants of rapamycin sensitivity in breast cancer cells. Clin Cancer Res 10:1013–1023

O'Reilly T, McSheehy PM (2010) Biomarker development for the clinical activity of the mTOR inhibitor everolimus (RAD001): processes, limitations, and further proposals. Transl Oncol 3:65–79

O'Reilly KE, Rojo F, She QB, Solit D, Mills GB, Smith D et al (2006) mTOR inhibition induces upstream receptor tyrosine kinase signaling and activates Akt. Cancer Res 66:1500–1508

Park SS, Kim SW (2007) Activated Akt signaling pathway in invasive ductal carcinoma of the breast: correlation with HER2 overexpression. Oncol Rep 18:139–143

Pattingre S, Espert L, Biard-Piechaczyk M, Codogno P (2008) Regulation of macroautophagy by mTOR and beclin 1 complexes. Biochimie 90:313–323

Peña-Llopis S, Vega-Rubin-de-Celis S, Schwartz JC, Wolff NC, Tran TA, Zou L, Xie XJ, Corey DR, Brugarolas J (2011) Regulation of TFEB and V-ATPases by mTORC1. EMBO J 30:3242–3258

Peng T, Golub TR, Sabatini DM (2002) The immunosuppressant rapamycin mimics a starvation-like signal distinct from amino acid and glucose deprivation. Mol Cell Biol 22:5575–5584

Possemato R, Marks KM, Shaul YD, Pacold ME, Kim D, Birsoy K, Sethumadhavan S, Woo HK, Jang HG, Jha AK, Chen WW, Barrett FG, Stransky N, Tsun ZY, Cowley GS, Barretina J, Kalaany NY, Hsu PP, Ottina K, Chan AM, Yuan B, Garraway LA, Root DE, Mino-Kenudson M, Brachtel EF, Driggers EM, Sabatini DM (2011) Functional genomics reveal that the serine synthesis pathway is essential in breast cancer. Nature 476:346–350

Raymond E, Alexandre J, Faivre S, Vera K, Materman E, Boni J et al (2004) Safety and pharmacokinetics of escalated doses of weekly intravenous infusion of CCI-779, a novel mTOR inhibitor, in patients with cancer. J Clin Oncol 22:2336–2347

Rojo F, Najera L, Lirola J, Jiménez J, Guzmán M, Sabadell MD et al (2007) 4E-Binding protein 1, a cell signaling hallmark in breast cancer that correlates with pathologic grade and prognosis. Clin Cancer Res 13:81–89

Rozenchan PB, Carraro DM, Brentani H, de Carvalho Mota LD, Bastos EP, e Ferreira EN, Torres CH, Katayama ML, Roela RA, Lyra EC, Soares FA, Folgueira MA, Góes JC, Brentani MM (2009) Reciprocal changes in gene expression profiles of cocultured breast epithelial cells and primary fibroblasts. Int J Cancer 125:2767–2777

Sabine VS, Sims AH, Macaskill EJ, Renshaw L, Thomas JS, Dixon JM et al (2010) Gene expression profiling of response to mTOR inhibitor everolimus in pre-operatively treated post-menopausal women with oestrogen receptor-positive breast cancer. Breast Cancer Res Treat 122:419–428

Satheesha S, Cookson VJ, Coleman LJ, Ingram N, Madhok B, Hanby AM, Suleman CA, Sabine VS, Macaskill EJ, Bartlett JM, Dixon JM, McElwaine JN, Hughes TA (2011) Response to mTOR inhibition: activity of eIF4E predicts sensitivity in cell lines and acquired changes in eIF4E regulation in breast cancer. Mol Cancer 10:19

Settembre C, Zoncu R, Medina DL, Vetrini F, Erdin S, Erdin S, Huynh T, Ferron M, Karsenty G, Vellard MC, Facchinetti V, Sabatini DM, Ballabio A (2012) A lysosome-to-nucleus signalling mechanism senses and regulates the lysosome via mTOR and TFEB. EMBO J 31:1095–1108

Sobral RA, Honda ST, Katayama ML, Brentani H, Brentani MM, Patrão DF, Folgueira MA (2008) Tumor slices as a model to evaluate doxorubicin in vitro treatment and expression of trios of genes PRSS11, MTSS1, CLPTM1 and PRSS11, MTSS1, SMYD2in canine mammary gland cancer. Acta Vet Scand 50:27

Sørlie T, Perou CM, Tibshirani R, Aas T, Geisler S, Johnsen H, Hastie T, Eisen MB, van de Rijn M, Jeffrey SS, Thorsen T, Quist H, Matese JC, Brown PO, Botstein D, Lønning PE, Børresen-Dale AL (2001) Gene expression patterns of breast carcinomas distinguish tumor subclasses with clinical implications. Proc Natl Acad Sci USA 98:10869–10874

Stoff-Khalili MA, Stoff A, Rivera AA, Banerjee NS, Everts M, Young S et al (2005) Preclinical evaluation of transcriptional targeting strategies for carcinoma of the breast in a tissue slice model system. Breast Cancer Res 7:1141–1152

Tabernero J, Rojo F, Calvo E, Burris H, Judson I, Hazell K, Martinelli E, Ramon y Cajal S, Jones S, Vidal L, Shand N, Macarulla T, Ramos FJ, Dimitrijevic S, Zoellner U, Tang P, Stumm M, Lane HA, Lebwohl D, Baselga J (2008) Dose- and schedule-dependent

inhibition of the mammalian target of rapamycin pathway with everolimus: a phase I tumor pharmacodynamic study in patients with advanced solid tumors. J Clin Oncol 26:1603–1610

Taylor IW, Linding R, Warde-Farley D, Liu Y, Pesquita C, Faria D, Bull S, Pawson T, Morris Q, Wrana JL (2009) Dynamic modularity in protein interaction networks predicts breast cancer outcome. Nat Biotechnol 27:199–204

Tokunaga E, Kimura Y, Oki E, Ueda N, Futatsugi M, Mashino K, Yamamoto M, Ikebe M, Kakeji Y, Baba H, Maehara Y (2006) Akt is frequently activated in HER2/neu-positive breast cancers and associated with poor prognosis among hormone-treated patients.Int J Cancer 118:284–289

Trapé AP, Katayama ML, Roela RA, Brentani H, Ravacci GR, de Araujo LL, Brentani MM (2012) Gene expression profile in response to doxorubicin-rapamycin combined treatment of HER-2-overexpressing human mammary epithelial cell lines. Mol Cancer Ther 11:464–474

Vaira V, Fedele G, Pyne S, Fasoli E, Zadra G, Bailey D, Snyder E, Faversani A, Coggi G, Flavin R, Bosari S, Loda M (2010) Preclinical model of organotypic culture for pharmacodynamic profiling of human tumors. Proc Natl Acad Sci USA 107:8352–8356

Vestey SB, Sen C, Calder CJ, Perks CM, Pignatelli M, Winters ZE (2005) Activated Akt expression in breast cancer: correlation with p53, Hdm2 and patient outcome. Eur J Cancer 41:1017–1025

Yoo YA, Kang MH, Kim JS, Oh SC (2008) Sonic hedgehog signaling promotes motility and invasiveness of gastric cancer cells through TGF-beta-mediated activation of the ALK5-smad 3 pathway. Carcinogenesis 29:480–490

Yu K, Toral-Barza L, Discafani C, Zhang WG, Skotnicki J, Frost P, Gibbons JJ (2001) mTOR, a novel target in breast cancer: the effect of CCI-779, an mTOR inhibitor, in preclinical models of breast cancer. Endocr Relat Cancer 8:(3)249–258

Zhou X, Tan M, Stone Hawthorne V, Klos KS, Lan KH, Yang Y et al (2004) Activation of the Akt/mammalian target of rapamycin/4E-BP1 pathway by ErbB2 overexpression predicts tumor progression in breast cancers. Clin Cancer Res 10:6779–6788

Zoncu R, Efeyan A, Sabatini DM (2011) mTOR: from growth signal integration to cancer, diabetes and ageing. Nat Rev Mol Cell Biol 12:21–35